manuscript No.
(will be inserted by the editor)

Diffusion modeling approach for time equilibration dialysis porewater sampler (DPS)

Vennin A. · Mesnage V. · Lecoq N.

Received: date / Accepted: date

Abstract To asses the water quality in estuaries nutrient fluxes at the sediment-water interface need to be measured. We developed an in situ method, the dialysis porewater sampler (DPS), which consists of a 30 cm-height plexiglass sheet in which fixed volume cells are regularly spaced of 1 cm and covered with a polysulfone membrane permeable to ions. Then the DPS is vertically insert into the sediment. Equilibration time may be long, ranging from 15 to 25 days. In order to optimise the equilibration time of the DPS, we developed a 1D diffusion model which considers the exchange between the sediment surrounding the cell and the dialysis cell itself. Both diffusive solute fluxes within the sediment and the permeable membrane towards the dialysis cell in a horizontal direction are considered. The physical parameters take into account in the diffusive model are : (i) diffusion coefficients of nutrient ions (N, P), (ii) tortuosity, (iii) permeation speed, (iv) initial concentration in the vertical direction. The sensitivity of the model to the physical/chemical parameters of the sediment such as porosity (or tortuosity), permeability of the membrane and temperature of the sediment is evaluated. Model's validation is realized with data obtained from muddy estuarine sediments (on the Seine river, Normandy, France). From a global point of view, the results of the 1D model calibration tested from field data highlight that the equilibration of the dialysis porewater sampler is not homogeneous on the 30 centimetres of sampled sediment column. Indeed, the results confirm the good correlation between

Vennin Arnaud
Normandie Universite, UMR CNRS 6143 M2C, Université de Rouen 76821 Mont-Saint-Aignan cedex, France E-mail: arnaud.vennin@etu.univ-rouen.fr

Mesnage Valérie
Normandie Université, UMR CNRS 6143 M2C, Université de Rouen 76821 Mont-Saint-Aignan cedex, France

Lecoq Nicolas
Normandie Université, UMR CNRS 6143 M2C, Université de Rouen 76821 Mont-Saint-Aignan cedex, France

the modelled and the measured profiles over the sediment depth except for the 5 first centimetres, whatever the ions considered (N or P). Then the model should to be improved by taking into account several physical parameters whose impact the first centimeters of sediment especially in dynamic ecosystems such as estuaries. But also biological parameters as bioturbation of the sediment-surface and/or by the activity of the micro-organisms consume the nutrients inside the cells. It is pointed out that parameters such as bioturbation rates or bacterial density must be integrated into this diffusion model in order to approach more precisely the environmental conditions.

Keywords Solute tranport · Porous medium · Fickian · Natural ecosystem · Diffusion modeling · Dialyser Porewater Sampler

1 Introduction

The assessment of water quality in natural ecosystem as estuaries, lagoons or lakes need to emphasize the chemistry of the two compartments of an aquatic ecosystem : (i) the water column and (ii) the sediment (Boström *et al.*, 1988; Sousa & Dangremond, 2011). Indeed natural ecosystem are favoured sites for the accumulation of fine organo-mineral particules and the sediment is known for its ability to store them (Boström *et al.*, 1988) at a certain period of the year and release them at others (Mesnage & Picot, 1995). Sediment compartment act as a sink by storing organic matter or as a source by releasing the nutrients after decomposition of bulk organic matter. Then the water-sediment interface represents the boundary of those two compartments : a porous medium (the sediment) and a liquid (the water column). Nutrients (C; N, P) fluxes have to be calculated in order to quantify the amount of C, N or P release from the sediment (Pasco & Baltz 2011). Nevertheless nutrient flux measurements are not easy due to the fluidity of the sediment interface and the hydrodynamic of the natural environment. Several techniques are available to sample sediment porewater (Sakho *et al*,. 2013). Some suggest a preliminary sediment-coring following with centrifugation or compression under nitrogen atmosphere to extract porewater. Others recommend the use of devices introduce into the sediment which after a given equilibration time allow for the sampling of porewater (Zhang *et al.*, 1999; Davison *et al.*, 2000; Leermakers *et al.*, 2005; Leermakers *et al.*, 2005; Xu *et al.*, 2012). We have previously developed this type of *in situ* method, the dialysis porewater sampler (DPS) of Hesslein type (Hesslein, 1976), which gives a continuous ion concentration profile of the sediment-water interface on 30 cm sediment-height, without massively disturbing the water-sediment interface. The dialysis device consists of a plexiglass sheet in which fixed volume cells are regularly spaced of 1 cm. A dialysis sampler has two columns of 40 cells; these are covered with a polysulfone membrane, permeable to major studied ions (Bally *et al.*, 2005). The dialysis porewater sampler is vertically insert into the sediment leaving several cells above the sediment-water interface and the others below. Equilibration time may lasts around 15 to 25 days according to the sediment characteristics,

but it allows its use in sediment estuaries subjected to strong hydrodynamic conditions. The dialysis porewater sampler remains in sediment during several tidal cycles (Bally *et al.*, 2004). As the equilibration time varies according to the sediment characteristics, it is necessary to re-estimate it in each studied ecosystem (Mesnage *et al.*, 2007, Dedieu *et al.*, 2007).

The aim of this work is to develop a full 1D diffusion model in order to estimate the optimal equilibration time and/or eventually to be able to calculate ion concentrations from results obtained in a short time (lower than the equilibration time). The conceptual model considers the exchange between the sediment surrounding the cell and the dialysis cell itself. Both diffusive solute fluxes within the sediment and the permeable membrane towards the dialysis cell in a horizontal direction are considered. The sensitivity of the model to the physical/chemical parameters of the sediment such as porosity (or tortuosity), membrane permeability (sorption/desorption) and sediment temperature were tested (Mesnage *et al.*, 2013).

2 Theory and calculation

2.1 Transport Equation in a Sediment Layer.

Pore-scale simulations are important because pore-scale phenomena have an major impact on larger scale and it is easier to systematically vary fluid properties, pore space geometries, and boundary conditions in computer simulations than in experiments. Although it is difficult to directly use results obtained from pore-scale simulations to improve quantitative predictions based on large-scale simulations, the understanding and information obtained from pore-scale investigations does contribute to our ability to understand large-scale natural processes and improve large-scale nutrient fluxes in ecosystem.

Therefore, we construct an equilibration model to simulate the equilibration of a DPS (dialysis pore-water sampler) embedded in sediment with an uniform pore-water concentration.
We used the following assumptions :

- the problem is treated in 1-dimensional, that is diffusion occurs only along the horizontal direction. This assumption will be validated later on by the concentration gradient estimation along the vertical direction. It should be smaller than the horizontal gradient of concentration.
- no-convection will be considered in the analysis; the Péclet number is assumed to be very small, and only diffusion of the major elements is considered.
- the solute concentration in a horizontal layer of sediment is constant, so the re-load by solid phase of the sediment has not been taken into account. This means that in the far field (far from the DPS), an uniform porewater concentration is considered.

A general formulation is presented first, special cases are treated in subsections thereafter.

We define the *outside* domain Ω_1 as the porous medium and the *inside* one Ω_2 the cell of the DPS (the DPS cell is initially filled with distilled water). Both domains are separated by a membrane of negligible thickness which allows ion transfer on both sides (no accumulate solutes on the membrane).
One-dimensional diffusion problem in porous medium (unsteady transport in the fluid phase) can be described when mass transport takes place in the direction of x-axis by the following time dependent differential equation :

$$\frac{\partial c_1}{\partial t} = -\frac{\partial}{\partial x}\left(J_c\right) \tag{1}$$

where J_c is the diffusion flux, c_1 is the solute concentration in the outside domain and t is the time. In the case of Fickian diffusion

$$J_c = -D^{eff}\frac{\partial c_1}{\partial x} \tag{2}$$

where D^{eff} is the "effective" diffusivity tensor of the solute in the bulk sediment, dependent upon the system's temperature, pressure and composition (Welty *et al.*, 1969) and is constant under the assumption that those parameters are time independent.

Because of the linearity of Fick's first law the size of the domain has no influence on the effective diffusion coefficient (at the larger-scale), and this coefficient is only a function of the pore geometry (and is independent of the applied concentration gradient) (Smith *et al.*, 2004; Mohajeri *et al.*, 2010). $(\partial c_1/\partial x)$ is the porewater concentration gradient.

Into the DPS cell (domain Ω_2), the one-dimensional diffusion equation is simply applied (classical diffusion in fluid with D_0 the diffusivity tensor in fluid).

The membrane is assumed to be a layer of negligible thickness. The flux across the membrane is proportional to the product of the permeation speed time the concentration difference across the membrane :

$$\frac{\partial c_i}{\partial t} = \frac{k^m}{F}\left(\frac{\partial c_i}{\partial x}\right)_{membrane} \tag{3}$$

where k^m is the permeation speed (assume to be a constant), F the form factor ($F = V/A$, where V and A are the volume and the membrane covered exchange area of the diffusion chamber, respectively).

By combining Eq.(1) and Eq.(2) and taking into account the effective diffusivity tensor definition, the following time-dependent differential equation for diffusion in the sediment becomes :

$$\frac{\partial c_1}{\partial t} = \frac{\partial}{\partial x}\left[D^{eff}\frac{\partial c_1}{\partial x}\right] \qquad \text{in } \Omega_1 \tag{4}$$

and in the DPS :

$$\frac{\partial c_2}{\partial t} = \frac{\partial}{\partial x}\left[D_0 \frac{\partial c_2}{\partial x}\right] \qquad \text{in } \Omega_2 \tag{5}$$

where c_1 and c_2 are specie concentration in domains 1 and 2 respectively. t is the time variable.

The boundaries and initial conditions are written in the form

$$c_1 = C_0 \text{ in } \Omega_1, \quad c_2 = 0 \text{ in } \Omega_2 \quad \text{for } t = 0 \tag{6}$$

$$\text{on } x = 0 \quad \frac{\partial c_2}{\partial x}.\mathbf{n} = 0 \quad \text{for } t \geq 0 \tag{7}$$

$$\text{on } x = l \quad \frac{\partial c_2}{\partial x}.\mathbf{n} = -k_m \left(c_1(x = l) - c_2(x = l)\right) \quad \text{for } t \geq 0 \tag{8}$$

$$x \to \infty \quad c_1 = C_0 \quad \text{for } t \geq 0 \tag{9}$$

where the DPS cell is in $x \in [0,\ l]$, $\mathbf{n}$ is the unit normal, and the porous medium is in $x \in [l,\ \infty[$. In Eq. (4), a source/sink term for the concentration of species can be added but it is neglected in this approach.

In Eq. (4) and in Eq. (5), the diffusion tensors are replaced by diffusion coefficients since we consider fluxes only along the x-direction.

2.1.1 Effective diffusion coefficients in porous media

The porous matrix complexity may lead to sub-diffusive transport in the porous medium. In addition to the specific interactions which may occur between the fluid phase and the solid medium (neglected in this approach), all the transport phenomena must take into account the decrease of the volume available to diffusion due to the presence of the solid medium and an increase of the path that ions must cross in the tortuous medium. These two effects can be described at a macroscopic level using the porosity and/or the tortuosity. Then diffusivity is lower in the porous medium than in free water.

Effective diffusion coefficient D^{eff} for anisotropic systems depends on the system geometry details but for isotropic systems it can be expressed as a function of the porosity alone (Kim *et al.*, 1987).

In the literature, three approaches are frequently used :

- Sediment diffusion coefficient D^{eff} (for effective diffusion) is derived from the equation

  $$D^{eff} = D_0 \times \phi$$

  where ϕ is the sediment porosity (e.g. Rosenberry *et al.*, 1985; Schuster *et al* , 2003) and D_0 is the diffusion coefficient for H^+ from Li and Gregory, (1974).
- In Jarvie *et al*, (2008), the bulk sediment diffusion coefficient D^{eff} was calculated from the tracer diffusion coefficient D_0 (Li and Gregory, 1974) and/or (Krom and Berner, 1980) using ϕ^2 for $\phi \leq 0.7$ and ϕ^3 for $\phi \geq 0.7$ (Ullman and Aller, 1982). A relation between the apparent diffusion coefficient of sediment and pore solution diffusion coefficient is given by

Bear and Bachmat (1991), Dormieux and Lemarchand (2001) and Smith *et al.* (2004) :

$$D_i = \phi \tau_i D_{0,i}, \quad \text{with} \quad \phi = \frac{V_f}{V_T} = \frac{V_T - V_S}{V_T}$$

where ϕ denotes the sediment porosity and $D_{0,i}$ is the self-diffusion coefficient of solute i in the pore fluid of the sediment (see Table 4 for typical values of self-diffusion coefficient of various ions). V_f, V_s, and V_T are the the fluid phase volume, the solid phase and the total sediment volume, respectively.
The (dimensionless) quantity τ_i is known as the tortuosity factor for the i-specie. In the case of uncharged porous media the tortuosity factor is a purely geometrical quantity characterizing the pore morphology (Bear and Bachmat, 1991). Values of τ_i ranges between 0 (impermeable pores) and 1 (cylindrical pores). For uncharged porous materials the tortuosity is the same for all diffusing species, i.e., $\tau_i = \tau =$ const.
One would notice that the product of τ and $D_{0,i}$ is often defined as the effective diffusion coefficient:

$$D_i^{eff} = \tau D_{0,i}$$

– The diffusivity is estimated by dividing the free-water value by the tortuosity squared τ^2 (Bally *et al.*, 2004; Bally *et al.*, 2005).

$$D^{eff} = \frac{D_0}{\tau^2} \tag{10}$$

This formulation is consistent with the previous relation of Bear and Bachmat (1991).

2.1.2 Tortuosity versus porosity

Whilst the porosity of a medium can be easily derived from weight and density in general the porous media tortuosity depends on pore volume fraction, shape and connectivity. However, for some class of materials, theoretical (or phenomenological) relations exists expressing the tortuosity as a function of the porosity only (Koponen *et al.*, 1997; Shen *et al.*, 2007; Boudreau, 1996).

Followong Faris *et al.* (1954) and Nelson and Simmons (1995) the relation of tortuosity in terms of porosity is usually described by Archie's (1942) law:

$$\tau^2 = \left(A\phi^{1-m}\right)^n \tag{11}$$

with three adjustable parameters A, m and n. These parameters are lithology-dependent. Relation (11) was used for sands (Lerman, 1979) and muds (Ullman and Aller, 1982) with $A = n = 1$ and m which may take several values (for instance, Bruggeman (1935) choose $m = 3/2$ for isotropic heterogeneous media and Millington and Quirk (1961) choose $m = 4/3$ for a homogeneous isotropic sphere packing media).

Other types of relations exist such as the linear function with one adjustable parameter :

$$\tau^2 = \phi + B(1-\phi) \tag{12}$$

used by Iversen and Jorgensen (1993) or the logarithmic function (Boudreau, 1996, Weissberg, 1963).

The best known among these expressions is Boudreau relation (Boudreau, 1996) :

$$\tau^2 = 1 - 2\ln(\phi) \tag{13}$$

This relation Eq.(13) is defined as the best least-squares fits of experimental data and is universally representative of the tortuosities in fine-grained unlithified sediments.

Recently, Du Plessis *et al* (2010) developed a deterministic 2D and 3D pore-scale model to predict diffusivity ratio of unconsolidated porous media in which diffusion process can be regarded as isotropic. Diffusivity ratio for fully staggered array of squares as a function of porosity obtained in this paper is in accordance with previous results as those of Kim *et al* (1987) and Quintard (1997).

The main relations are summarized in table 4.

2.1.3 Porosity and compaction of the media

By changing properties of ϕ (and consequently of τ^2) the following equation describes the functional dependency on the vertical z-direction due to compaction of the porous media. Thereafter, it is assumed (Boudreau, 1997; Burdige, 2006; Holzbecher, 2004; Reed *et al.*, 2011) that an exponential relation holds for porosity :

$$\phi(z) = \phi_\infty + (\phi_0 - \phi_\infty)\exp(z/\lambda) \tag{14}$$

with the situation $z \leq 0$ with $z = 0$ is the interface fluid-porous medium. ϕ_0 and ϕ_∞ are respectively porosities at the interface fluid-sediment and at depth. λ is a parameter describing the dependency on z; taking $\lambda = 0$ gives a constant porosity and tortuosity; for $\lambda > 0$, the porosity decreases with a decreasing value of z, and this may model the compaction of the sediment. This approach is consistent with experimental results in which porosity profiles typically exhibit a smooth and regular shape in the upper few decimetres of marine sediments and reach a constant value at depth (Burdige, 2006; Boudreau and Bennett, 1999; Mulsow *et al.*, 1998).

2.1.4 Dimensionless equations

In order to homogenize, all the variables will be normalised with respect to the characteristic length l, concentration at infinity C_0 and diffusion in free-water D_0.

Let us introduce the following representation of the dimensional variables appearing in Eqs. (4)-(9) where the overline ˜ denotes dimensionless variables

$$\tilde{c_i} = \frac{c_i}{C_0} \quad i = 1, 2, \qquad \tilde{t} = \frac{D_0 t}{l^2}, \qquad \tilde{x} = \frac{x}{l} \tag{15}$$

The governing equations take the following form :

$$\frac{\partial \tilde{c_1}}{\partial \tilde{t}} = \frac{1}{\tau^2} \frac{\partial^2 \tilde{c_1}}{\partial \tilde{x}^2} \qquad \text{in } \Omega_1 \tag{16}$$

and in the DPS :

$$\frac{\partial \tilde{c_2}}{\partial \tilde{t}} = \frac{\partial^2 \tilde{c_2}}{\partial \tilde{x}^2} \qquad \text{in } \Omega_2 \tag{17}$$

and the boundary condition :

$$\tilde{c_1} = 1 \text{ in } \Omega_1 \quad \tilde{c_2} = 0 \text{ in } \Omega_2 \quad \text{for } \tilde{t} = 0 \tag{18}$$

$$\text{on } \tilde{x} = 0 \quad \frac{\partial \tilde{c_2}}{\partial \tilde{x}} . \mathbf{n} = 0 \quad \text{for } \tilde{t} \geq 0 \tag{19}$$

$$\text{on } \tilde{x} = 1 \quad \frac{\partial \tilde{c_2}}{\partial \tilde{x}} . \mathbf{n} = -\tilde{k_m} \left(\tilde{c_1}(\tilde{x} = 1) - \tilde{c_2}(\tilde{x} = 1) \right) \tag{20}$$

$$\tilde{x} \to \infty \quad \tilde{c_1} = 1 \tag{21}$$

It should be noticed that the mathematical model Eqs. (16)-(21) is one-dimensional. The accuracy of this natural approximation can be readily justified by the fact that concentration gradients in the porous medium adjacent to the DPS in horizontal direction (x-direction) are much greater than gradients along the vertical direction (z-direction). This could be understand by the fact that sediments are deposited in horizontal layers without vertical mixing in the bottom layers. Thus, the coefficient of diffusion D^{eff} must be replaced by a tensor which should be diagonal (Lecoq *et al.*, 2008) with coefficient along the z-direction lower than the one in the x-direction. This assumption will be validated "a posteriori" by calculating fluxes in all directions under the assumption of equal coefficient of diffusion (see subsection 3.1.3 for more details).

2.2 Numerical method and parameters

The model outlined above is solved numerically using the method of finite differences in times and positions. An explicit formulation is used which implies that the CFL condition (Courant-Friedrichs-Lewy) is satisfied (adaptative time-step method). The length of the porous media is chosen to L=100xl with l=1 so that no boundary effects are visible (Mesnage et al 2013). Simulations were performed with a 10^6 normalised time steps, which corresponds roughly to 30 days for the ammonium ion for instance.

The tortuosity is estimated with the formulations of Archie (1942) or Boudreau (1996) given previously respectively in Eq.(11) and Eq.(13).

In this work, the third approach is applied for the effective diffusion coefficient estimation Eq.(10) and the effect of porosity change given by Eq. (14) with different data sets are used (see section 2.3).

2.3 Porosity and concentration models used

As explained above, several parameters like porosity and concentration of ions may depend on the vertical z-direction. For easier reading, we decompose the problem into two sub-problems, one with constant porosity and the other with variable porosity along the vertical z-direction.

*2.3.1 Constant-Porosity Model (***CPM***) versus Variable-Porosity Model (***VPM***)*

First we consider the case of porosity ϕ and consequently tortuosity τ which are homogeneous in the vertical z-direction. This assumption is validated by many experiments and modelling described in the literature as for instance Bally *et al* (2004; 2005), Grigg (1999), Mao *et al* (2006). The porosity is assumed to be equal to 0.62, which corresponds to the mean value obtained in the pore-water of an intertidal mudflat of the Seine Estuary (the data of this site will be used for comparison with the model later).

Similarly as for the constant-porosity model, we introduce the dimensionless, depth-dependent porosity model (VPM). The porosity is given previously by Eq.(14), the unknown parameters ϕ_0, ϕ_∞, and λ are extracted from the shape of the expected curve and the mean value over the depth. The average values of both approaches are assumed to be exactly the same as from the experimental reference, that is $< \phi >= 0.62$.

Fig. 1 (a.) presents the porosity versus the normalised depth into the sediment. The origin $\tilde{z} = 0$ is the water-sediment interface.

The vertical line corresponds to a constant porosity with depth (**CPM**).

The most simple model is to assume a linear dependence of ϕ with the depth $\tilde{z}$ into the sediment. This case is not treated in this approach since it is purely a simplification of the cases presented below. The curves in Fig. 1 (a.) correspond the **VPM** approch, it corresponds to the porosity describe by Eq.(14).They come from *in situ* porosity measures (Bally et al., 2004). It presents an exponential decrease with depth due to the biogenic mixing in the uppper layers and a compaction of sediment in the lower layers mixing named bioturbation; this approach takes into account the decline in faunal density with increasing depth into the sediment (Boudreau, 1986).

Then bioturbation is modelled as a diffusive process modification representing random small-scale displacement of particles and pore water by benthic fauna (Goldberg and Koide, 1962; Guinasso and Schink, 1975; Boudreau, 1986). In Kim *et al.*(1987), it is shown that the anisotropic systems geometry details exert an important influence on effective transport coefficients.

2.3.2 Initial concentration profil

The normalised concentration profiles are presented on Fig. 1 (b). The parameters and studied cases are summarized in table 4. The term "like" refers to the concentration profile provided by field data for the considering element. They have been implemented in the model to see how it changes the diffusion in the sediment. Three elements are considered two because they are important in the estaurian ecosystem: phosphorus and ammonium and one because of its inert propriety in regards of the sediment (no sorption/desorption effect).

3 Results and discussion

3.1 Theoretical results

3.1.1 Tortuosity models

The sediment is composed of particles of different sizes and shapes which impact the space geometry in the porous media. Therefore ions do not diffuse in the sediment by following straight lines but are deviated by the particles. Consequently the diffusion coefficient is modified to be taken into account in the models. Models from the literature for predicting the diffusivity ratio in porous media involving isotropic diffusion processes can be classified into two categories : Boudreau and Archie models. A comparison between the various tortuosity models and its influence on the ions diffusion is shown in Fig. 2. The diffusion model given by Eq. (16-21) was applied to study the equilibration of the DPS under initial conditions of constant porosity and concentration with depth, but the models used to estimate tortuosity from porosity follow Boudreau or Archie laws. The tortuosity equations used are those proposed by Boudreau (1986) and by Archie (1942) named respectively CPM_1 and CPM_2 (table 2).

Equilibration ranges from 0 to 1, with 1 corresponding to full equilibration of the DPS in other words the concentration inside the DPS is equal to concentration into the sediment. Applying Fick's law, it needs an infinite time to achieve the sediment concentration into the DPS.

On Fig. 2, the two curves appear to be close to each other, the concentration in the reference cell evolves in the same way. However by looking at the enlargement on Fig. 2, the delay is estimated to 10.10^3 or 15.10^3 time-step units. Considering the case of equal porosity ($< \phi >= 0.62$ in our case), a small difference in tortuosity leads to a delay of 2.5 time units, that is a relative difference of 8% to obtain the same normalised concentration $\tilde{c} = 0.9$. If we consider a same normalised concentration $\tilde{c} = 0.5$, then the relative difference decrease to 4%.

For instance, considering the most diffusing ion of interest NH_4^+, the diffusion coefficient in pure water is estimated to $D_0(NH_4^+)(T = 25^oC) = 19.8\ 10^{-6}\ cm^2 s^{-1}$ (Li and Gregory, 1974) and a reference cell of size $l = 10^{-2}$

m. Eq. 16 is used to estimate the delay time, that is :

$$t = \frac{l^2 \tilde{t}}{D_0}$$

For a normalised concentration $\tilde{c}$ equal to 0.5, the delay reaches the value of 40 minutes, whereas for $\tilde{c} = 0.9$, the delay increases up to 18 hours which in fact represents a noticeable difference in the equilibration dynamic.

On Fig. 3 it is plotted the concentration difference between CPM_1 and CPM_2 over time. The maximum of difference occurs at the beginning of the diffusion around $1.5.10^5$ time-steps and then decreases. However by looking at the y axis it reveals that all over the time the difference stays at a low level to reach a maximum value of $8.0.10^{-3}$. Despite the gap in time between results obtained with Archie and Boudreau formulation, the concentration are similar and the difference is negligible. Furthermore this difference cannot be distinguished due to the chemical precision analysis (see below figure 6) this range precision is included within the errorbars.

Accordingly the two tortuosity equations lead to the conclusion that there is no significative difference between Archie and Boudreau equations. The curves for the normalised concentration seem very similar in spite of the delay in time which can only reach a difference up to less than 1 day for 90% of equilibration. Therefore Boudreau's equation will be used for the rest of the study. This decision is motivated by the fact that the latter equation is the most commonly used in a large range of publications which allow them to make comparaison with other publications and is regarded widely as a good tortuosity estimation.

3.1.2 Porosity profile with depth

The porous media does not have a homogeneous space symmetry with depth. Deeper the particles are, the stronger the pressure created by its own weight is. Hence the porosity and thus the tortuosity will change with depth.

The impact of this physical phenomenon is evaluated in the model by considering VPM_1 (table 2) which consist of a decreasing porosity with depth and a homogeneous ion concentration to show the porosity contribution in the diffusion dynamic. Figure 4 shows VPM_1 with three curves for three different normalised depths such as 0, 0.5 and 1 named respectively top, middle and bottom layers. The top layer reaches a 0,9 value of equilibration faster than the other layers.

The sediment porosity variation on the contrary to the tortuosity law has an important impact on the equilibration time of the DPS. It stands out that the diffusion is lower in the bottom layers than on the top layers when considering a decreasing variable porosity with depth in the sediment. This is

a key result that to obtain a realistic modelling of the equilibration time of the DPS, porosity variation has to be taken into account. Different porosity profiles and thus different environments will change the necessary time for the DPS to reach the equilibration. On the field, this variation is due to the fact that the particles fall in the water column, reach the surface of sediment and start to be buried. As this phenomena occurs the burial result is an increase of compaction and a decrease of space between each particle which ends with a lower sediment porosity. This quick change of porosity has been showed on the scale of the DPS (i.e. 30 centimetres depth) for an estuary (Wheatcroft *et al.*,2013).

3.1.3 Concentration gradient nearby the DPS

During the diffusion in the sediment, the ion concentration is modified when passing through the porous media to the cell. This modification creates areas where concentrations are greater and as a consequence areas where concentrations are lower. This induces what is called concentration gradients. The gradients are plotted considering on a vertical slice of sediment. The outputs are computed to give from red to blue a scale where the red represents the high gradient and in blue the low gradients. The large area on the left of the vertical profile (Fig 5) is the sediment and the narrow part split up on the right represents the DPS. Gradients come from the following formula:

$$\| \nabla c \| = \sqrt{\left(\frac{\partial c}{\partial x}\right)^2 + \left(\frac{\partial c}{\partial y}\right)^2}$$

The gradients are plotted on x and y direction separately to appreciate in which direction they occur. There are four cases considered: VPM_1, VPM_2, VPM_3, VPM_4 as described in table 2. VPM1 is set to include only a decreasing porosity variation with depth and homogeneous concentration within the sediment slices. The gradients on x are concentrated vertically nearby the DPS slightly curved on the bottom part. On y axis gradients are concentrated on the bottom. The magnitude (product of x and y gradients) shows an upside down T shape close to the DPS.

On the three others VPM 2, 3 and 4 are represented and respectively show the ammonium, phosphorus and bromium concentration in the porous medium as on fig 1. In fact those cases exhibit the same pattern considering both x and y direction. On x the highest gradients concentrate on the bottom of the profile nearby the sediment. However they are different in size. On VPM_4 gradients spread over the entire depth of the profile and less on VPM_2. On y-axis gradients are horizontal but are similar on the three cases the wider is VPM_2 which presents a gradient over the entire profile unlike VPM_4 which only shows a gradient at the top of the profile. Concerning the magnitude it shows only a horizontal gradient which results in the product of both x and y direction. VPM_1 shows how the porosity variation acts on the gradients. When the porosity decreases the area covers by the gradients increases. The

decrease of porosity is offset by the enlargement of the gradient area. This phenomenon is observed on every case but the difference lie on the y-axis contribution. The bigger the y-axis vertical gradients on the upper part the larger the vertical gradient on x. The difference between case VPM 2, 3, 4 results from the concentration arrays put in the model namely the shape of the element concentration with depth (fig 1). The concentration slope of the considering element induces bigger gradient on y if the slope is steeper.

Thus in the sediment there are horizontal gradients such as hypothesized but also vertical gradients. Those y-axis gradients are dominant factors in the diffusion dynamic therefore unlike the hypothesis stated the vertical gradients have to be taken into account and introduce into the model to allow it to be more accurate. The gradients study allows also to demonstrate that every nutrient will have a different behaviour due to its concentration profile within the sediment. The working range of each of them is different, deeper for the ammonium than the bromium for instance.

3.2 Model validation with *in situ* data set

Three ions are considered: ammonium and phosphorus are called nutrients because they are involve in the micro-organisms and plants nutrition processes. Bromium is also considered due to its conservative behavior which means that it does not interact with the porous media or micro-organisms contrarily to the precedent ions. The data come from a field work on mudflats at the Seine River mouth (Bally *et al.*, 2004). The concentration with depth of those ions in the DPS cells for two different equilibrium data profiles in the sediment (data set 1 and 2) are represented on figure 6 (a,c,e). Error bars coming from the data series standard deviation are added. The theoretical profiles (named Model $\phi = 0.62$ and $< \phi >= 0.62$ on the graph) are the model outputs with two porosity profiles with depth. A first one with a constant porosity of 0.62 with depth and a second one with a variable porosity with depth which have a mean porosity of 0.62. Only one data curve is represented about bromium because it is represented by one set of data and so does not allow to calculate standard deviation. It results in a lack of relevance for this datum. For the major part on the three graph a,c,e (fig.6) the data set 1 and 2 and the model outputs (constant and variable porosity over depth) are situated within the error bars therefore the model is in good agreement with the diffusion phenomenon between the DPS and the sediment porewater. Nevertheless the correlation coefficients are regrouped in table 3 and confirms that the model outputs fit well the data. However the data curves do not fit the model curves by focusing on the 5 first centimetres at the water/sediment interface for ammonium and phosphate. It can be explained by the fact that the model does not take into account the phenomena which occur at the water/sediment interface such as bioturbation or hydrodynamic forcing.

On figure 6 (graph b,d,f) are also represented for each ions the theoretical evolution of the concentration in the DPS cells for 4 time-steps (2.10^5, 5.10^5, 10.10^5, 15.10^5). The concentration shape with depth is different for the three different ions. It involves different diffusion behaviours in the porous media but also with the overlying water. By looking at the 5 first centimetres the curve slope is steeper concerning the ammonium or the phosphate than for the bromium. Furthermore the gap between the concentration at 2.10^5 time-steps and 15.10^5 time-steps at the interface for the bromium is more important than for ammonium or phosphate. This shows that a bigger concentration causes a bigger diffusion dynamic within the sediment. It will result in different fluxes.

Thus the model is relevant to simulate the DPS equilibration. However the model should be improved by considering phenomenon which occur at the water/sediment interface such as adsorption or bioturbation. This area is important because this is where the ion exchanges occur with the overlying water. Thus to obtain a good estimation of the fluxes more parameters should be added.

4 Conclusion

This study underlines the main parameters that should be considered to predict the equilibration time between the sediment and the DPS. The goal is to reduce the residence time of the device within the sediment which permit to reduce the duration of the fieldwork. It found out that the main parameter that control the equilibration time is the porosity profile with depth, nutrient concentrations within the sediment does not contribute. This study not only permit to improve the method of the DPS but also permit to study the mechanisms which occur in the sediment and will be useful to achieve an another goal of this study: calculate nutrient fluxes between the sediment and the overlying water in the Seine River estuary. Now our study should focus on the other parameters which should be added in the model such as bioturbation which impacts the first centimetres of the sediment by changing porosity profile, specific phenomenon which occurs just for specific ions like adsorption/desorption for phosphates and study other compounds like organic carbon to study the carbon sink/source of mudflats. By changing those parameters we allow the model to be suitable for extensive kind of environments such as a mangrove in tropical climate or other climatic areas.

References

1. Archie, G. E. (1942). The electrical resistivity log as an aid in determining some reservoir characteristics. Transactions of the AIME, 146(01), 54–62.
2. Bally, G., Mesnage, V., Deloffre, J., Clarisse, O., Lafite, R., Dupont, J. P. (2004). Chemical characterization of porewaters in an intertidal mudflat of the Seine estuary: relationship to erosiondeposition cycles. Marine Pollution Bulletin, 49(3), 163-173.
3. Bally, G., Mesnage, V., Verney, R., Clarisse, O., Dupont, J-P., Ouddanne, B., Lafite, R., 2005. Dialysis porewater sampler: a strategy for time equilibration optimization. In: Seranno, L., Golterman, H.L. (Eds.), Phosphates in Sediments, Proceedings of the 4th International Symposium. Backhuys, The Netherlands, pp. 9–20.
4. Bear, J., Bachmat, Y. (1990). Introduction to modeling of transport phenomena in porous media (Vol. 4). Springer Science & Business Media.
5. Bostroḿ, B., Andersen, J. M., Fleischer, S., Jansson, M. (1988). Exchange of phosphorus across the sediment-water interface. In Phosphorus in Freshwater Ecosystems (pp. 229-244). Springer Netherlands.
6. Boudreau, B.P. 1986. Mathematics of tracer mixing in sediments : 1. Spatially-dependent, diffusive mixing. American Journal of Science 286: 161–198.
7. Boudreau, B. P. (1996). The diffusive tortuosity of fine-grained unlithified sediments. Geochimica et Cosmochimica Acta, 60(16), 3139-3142.
8. Boudreau, B. P. (1997). Diagenetic models and their implementation (Vol. 505). Berlin: Springer.
9. Boudreau, B. P., Bennett, R. H. (1999). New rheological and porosity equations for steady-state compaction. American Journal of Science, 299(7-9), 517-528.
10. Bruggemann, D.A., 1935. Berechnung verschiedener physicalisher konstate von heterogen substanzen. Annal der Physik 24, 636–664.
11. Burdige, D. J. (2006). Geochemistry of marine sediments (Vol. 398). Princeton: Princeton University Press.
12. Davison, W., Fones, GR., Harper, M., Teasdale, P., Zhang, H., 2000. Dialysis, DET and DGT: in situ diffusional techniques for studying water, sediments and soil. In: Buffle J, Horvai G, editors. In situ monitoring of aquatic systems: chemical analysis and speciation. IUPAC. England: John Wiley & Sons Ltd. p. 495569.
13. Dedieu K., Rabouille C., Thouzeau G., Jean F., Chauvaud L., Clavier J., Mesnage V., Ogier S., 2007. Benthic O2 distribution and dynamics in a Mediterranen lagoon (Thau, France): An in-situ microelectrode study. Estuarine Coastal and Shelf Sciences. **72**, 393-405.
14. Dormieux, L., Lemarchand, E. (2001). Homogenization approach of advection and diffusion in cracked porous material. Journal of engineering mechanics, 127(12), 1267-1274.
15. du Plessis, E., Woudberg, S., du Plessis, J. P. (2010). Pore-scale modelling of diffusion in unconsolidated porous structures. Chemical Engineering Science, 65(8), 2541-2551.
16. Faris, S.R., Gournay, L.S., Lipson, L.B., Webb, T.S., 1954. Verification of tortuosity equations. AAPG Bulletin 38, 2226–2232.
17. Goldberg, E. D., Koide, M. (1962). Geochronological studies of deep sea sediments by the ionium/thorium method. Geochimica et cosmochimica acta, 26(3), 417-450.
18. Grigg, N.J. 1999. Pore-water convection induced by peeper emplacement in saline sediment. Limmol. Oceanogr. 42 (2), 425–430.
19. Guédron, S., Huguet, L., Vignati, D.A.L., Liu, B., Gimbert, F., Ferrari, B.J.D., Zonta, R., Dominik, J. 2012. Tidal cycling of mercury and methylmercury between sediments and water column in the Venice Lagoon (Italy). Marine Chemistry 130-131, 1-11.
20. Guinasso, N. L., Schink, D. R. (1975). Quantitative estimates of biological mixing rates in abyssal sediments. Journal of Geophysical Research, 80(21), 3032-3043.
21. Hesslein, R. H., 1976. An in situ sampler for close interval porewater studies. Limnology and Oceanography, 21(6), 912914.
22. Holzbecher, E. 2004. Mathematical analysis of the effect of sedimentation and compaction on steady transport profiles in sediments. Transport in Porous Media 57: 279–296
23. Iversen, N., Jrgensen, B. B. (1993). Diffusion coefficients of sulfate and methane in marine sediments: Influence of porosity. Geochimica et Cosmochimica Acta, 57(3), 571-578.

24. Jarvie, H. P., Mortimer, R. J., Palmer-Felgate, E. J., Quinton, K. S., Harman, S. A., Carbo, P. (2008). Measurement of soluble reactive phosphorus concentration profiles and fluxes in river-bed sediments using DET gel probes. Journal of hydrology, 350(3), 261-273.
25. Kim, J. Ochoa, J.A. and Whitaker, S. 1987. Diffusion in anisotropic media. Transport in Porous Media 2, 327–356.
26. Koponen, A., Kataja, M., Timonen, J. (1997). Permeability and effective porosity of porous media. Physical Review E, 56(3), 3319.
27. Krom, M.D. and Berner R.A. 1980. The diffusion coefficients of sulfate, ammonium, and phosphate ions in anoxic marine sediments. Limnol. Oceanogr. 25(2), 327–337.
28. Lecoq, N., Boisse, J., Patte, R., and Zapolsky, H. 2008. Coarsening Kinetic of Aluminium-Scandium and Aluminium-Zirconium-Scandium Precipitates. In ICAA'11, Aachen, September 2008, Aluminium Alloys : Their Physical and Mechanical Properties Edited by J. Hirsch, B. Skrotzki and G. Gottstein, Wiley-VCH GmbH & Co. KgaA.
29. Leermakers, M., Gao, Y., Gabelle, C., Lojen, S., Ouddane, B., Wartel, M., Baeyens, W., 2005. Determination of high resolution porewater profiles of trace metals in sediments of the rupel river (Belgium) using DET (Diffusive Equilibration in Thin Films) and DGT (Diffusive Gradients in Thin Films) techniques. Water, Air, and Soil Pollution 166, 265286.
30. Lerman, A., 1979. Geochemical processes: water and sediment environments. Wiley, New-York.
31. Li, Y.H. and Gregory, S. 1974. Diffusion of ions in sea water and in deep-sea sediments. Geochim. Cosmochim. Acta. 38, 708–714.
32. Mao, X., Enot, P., Barry, D.A., Li, L., Binley, A. and Jeng, D.S. 2006. Tidal influence on behaviour of a coastal aquifer adjacent to a low-relief estuary. J. Hydrol. **327** 110–127.
33. Malcom, S. J., and Sivyer, D.B. 1997. Nutrient recycling intertidal sediments. In Biogeochemistry of intertidal sediments. Cambridge environmental chemistry series (9). Eds. Jickells T.D. & Rae J.E. Cambridge University press. 84-96.
34. Mesnage, V., Lecoq, N., Sakho, I., Vennin, A. (2013). Modeling nutrients profiles at the sedimentwater interface. Calibration and validation from two climatically contrasted estuaries: Seine (France) and Somone (Senegal). Comptes Rendus Geoscience, 345(11), 439-445.
35. Mesnage, V., Ogier S., Bally, G., Disnar, J-R., Lottier, N., Dedieu, K., Rabouille, C., Copard, Y., 2007. Nutrient dynamics at the sedimentwater interface in a Mediterranean lagoon (Thau, France): Influence of biodeposition by shellfish farming activities. Marine Environmental Research 63, 257277.
36. Milington, R.J. and Quirk, J.P., 1961. Permeability of porous solids. Trans. Faraday. Soc. 57, 1200–1207.
37. Mohajeri, A., Narsilio, G., Pivonka, P., Smith, P. 2010. Numerical estimation of effective diffusion coefficients for charged porous materials based on micro-scale analyses. Computers and Geotechnics 37, 280–287.
38. Mulsow, S., Boudreau, B.P., Smith, J.N. 1998. Bioturbation and porosity gradients. Limnol. Oceanogr. 43, 1–9.
39. Nelson, J.S., Simmons, E.C., 1995. Diffusion of methane and ethane through the reservoir cap rock : implications for the timming and duration of catagenesis. AAPG Bulletin 79, 1064–1074.
40. Pascot:2011) Pasco, T.E., Baltz, D.M., 2011. Trophic relationships in salt marshes of coastal and estuarine ecosystems. Trophic Relationships of Coastal and Estuarine Ecosystems 6, 261269.
41. Powers, S.E., Loureiro, C.O., Abriola, L.M. and Weber W.J. 1991. Theoretical study of the significance of non equilibrium dissolution of nonaquaeous phase liquids in subsurface systems. Water Ressources Research 27(4), 463–477.
42. Quintard, M., Kaviany, M. and Whitaker, S. 1997. Two-medium treatment of heat transfer in porous media: numerical results for effective properties. Advances in Water Resources 20, Nos 2-3, 77–94.
43. Reed, D.C., Slomp C.P. and Gustafsson B.G. 2011. Sedimentary phosphorus dynamics and the evolution of bottom-water hypoxia: A coupled benthic-pelagic model of a coastal system. Limmol. Oceanogr. 56(3), 1075–1092.

44. Rosenberry DO. 1985. Factors contributing to the formation of transient water-table mounds on the outflow side of a seepage lake, Williams Lake, Central Minnesota. MS thesis, University of Minnesota, Minneapolis: 127 pp.
45. Sakho I., Mesnage V., Lecoq N., Lafite R. Deloffre J. 2013. Biogeochemistry study in mangrove ecosystem sediments using dialysis porewater sampler. In Mangrove Ecosystems: Biogeography, genetic Diversity and conservation strategies. Chapter 9. Environmental Research Advances Series. (Ed .) G. Gleason & T.R. Victor. (Pub.) Nova Sciences. 167-189.
46. Sousa, W.P., Dangremond, E.M., 2011. Trophic interactions in coastal and estuarine mangrove forest ecosystems. Reference Module in Earth Systems and Environmental Sciences 6, 43-93.
47. Schuster, P., Reddy, M., LaBaugh, J., Parkhurst, R., Rosenberry, D., Winter, T., Antweiler, R., Dean, W. 2003. Characterization of lake water and ground water movement in the littoral zone of Williams Lake, a closed-basin lake in north central Minnesota, Hydrol. Process. 17, 823838
48. Shen, L., Chen, Z. 2007. Critical review of the impact of tortuosity on diffusion. Chem. Eng. Sci. 62, 3748–3755.
49. Smith, D., Pivonka, P., Jungnickel, C., Fityus, S. 2004. Theoretical Analysis of Anion Exclusion and Diffusive Transport Through Platy-Clay Soils. Transport in Porous Media 57: 251–277.
50. Sundby B., Gobeil C. Silverberg N., Mucci A. 1992. The phosphorus cycle in coastal marine sediments. Limnology and Oceanography. **37**(6). 1129-1145.
51. Ullman, W.J., Aller, R.C., 1982. Diffusion coefficients in near shore marine sediments. Limnology Oceanography 27, 552–556.
52. Wheatcroft, R. A., Sanders, R. D., Law, B. A. 2013. Seasonal variation in physical and biological factors that influence sediment porosity on a temperate mudflat: Willapa Bay, Washington, USA. Continental Shelf Research, 60, S173-S184.
53. Weissberg, H., 1963. Effective diffusion coefficient in porous media. Journal of Applied Physics 34, 2636–2639.
54. Welty, J. R., Wicks, C. E., Rorrer, G., Wilson, R. E. (2009). Fundamentals of momentum, heat, and mass transfer. John Wiley & Sons.
55. Xu, D., Ding, S., Sun, Q., Zhong, J., Wu, W., Jia, F., 2012. Evaluation of in situ capping with clean soils to control phosphate release from sediments. *Science of The Total Environment* 438, 334–341.

Relation	Parameters	Media	References
$\tau^2 = (A\phi^{1-m})^n$	A, m and n	Sands	Lerman, (1979)
		Muds	Ullman and Aller, (1982)
	$A = n = 1, m = 3/2$	Spheres	Bruggeman (1935)
	$A = n = 1, m = 1.4$	Arrays of squares	Du Plessis *et al* (2010)
	$A = n = 1, m = 2.14$	Sediments	Archie (1942)
$\tau^2 = \phi + B(1-\phi)$	B	Soils	Iversen and Jorgensen (1993)
$\tau^2 = 1 - C\ln(\phi)$	C	sediments	Boudreau (1996) Weissberg (1963)
$\tau^2 = 1 - 2\ln(\phi)$		unlithified sediments	Boudreau (1996)

Table 1 Tortuosity-porosity relations mainly used in the literature

Case	Porosity	Tortuosity equation	Concentration profile
CPM_1	constant $\phi = 0.62$	Boudreau (1986)	constant
CPM_2	constant $\phi = 0.62$	Archie (1942)	constant
VPM_1	variable $< \phi >= 0,62$	Boudreau (1986)	constant
VPM_2	variable $< \phi >= 0.62$	Boudreau (1986)	ammonium-like
VPM_3	variable $< \phi >= 0.62$	Boudreau (1986)	phosphate-like
VPM_4	variable $< \phi >= 0.62$	Boudreau (1986)	bromium-like

Table 2 Cases considering in the study

Ion	Porosity	Data Set 1	Data Set 2
NH^{4+}	constant	0.73	0.88
NH_4^+	variable	0.73	0.89
PO_4^{2-}	constant	0.98	0.99
PO_4^{2-}	constant	0.98	0.99
Br^-	constant	0.27	0.97
Br^-	variable	0.24	0.96

Table 3 Correlation coefficient between the data set 1 and 2 and the model outputs with or without variable porosity

Parameter	Values used into the model	Units
Diffusion coefficients		
D_0 (NH_4^+) $(T = 11^o\ C)$	13,2	$10^{-6}\ cm^2.s^{-1}$
D_0 (PO_4^{2-}) $(T = 11^o\ C)$	4,9	$10^{-6}\ cm^2.s^{-1}$
D_0 (Br^-) $(T = 11^o\ C)$	14,2	$10^{-6}\ cm^2.s^{-1}$
Tortuosity		
τ^2	1.96 – 2.25	
Permeation speed		
k^m	0.43	$m.s^{-1}$
Dynamic viscosity of water		
η $(T = 11^o\ C)$	0.0001271	$kg.s.m^{-1}$
Equilibrium concentration		
$C_0(SO_4^{2-})$	2000–2500	$mg.l^{-1}$
$C_0(Ca^{2+})$	400–500	$mg.l^{-1}$
$C_0(Mg^{2+})$	1200–1500	$mg.l^{-1}$

Table 4 Physical parameters used in the model Eqs. 15–21

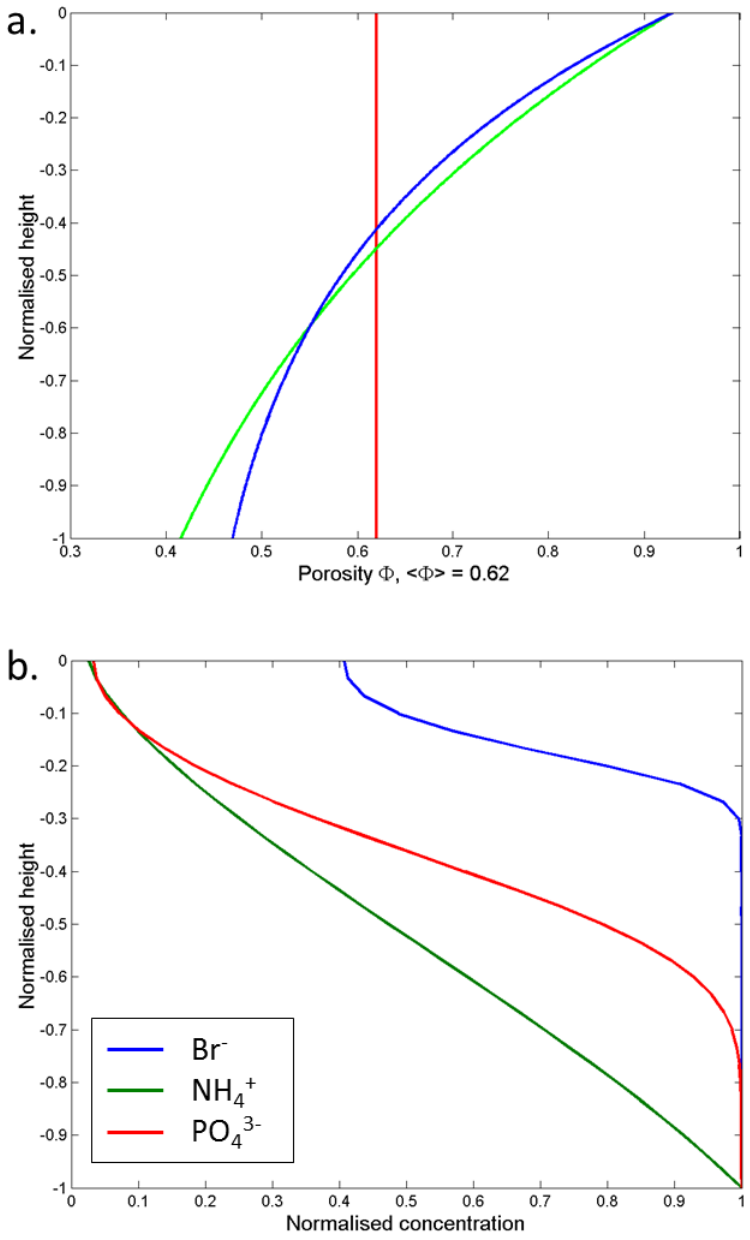

Fig. 1 Porosity over normalised depth profils considered in the study (the mean value over the depth is equal to 0.62) (a). Normalised concentration profile over normalised depth for ammonium, phosphate and bromium (b). These profiles are used in the numerical model **CPM** and **VPM**.

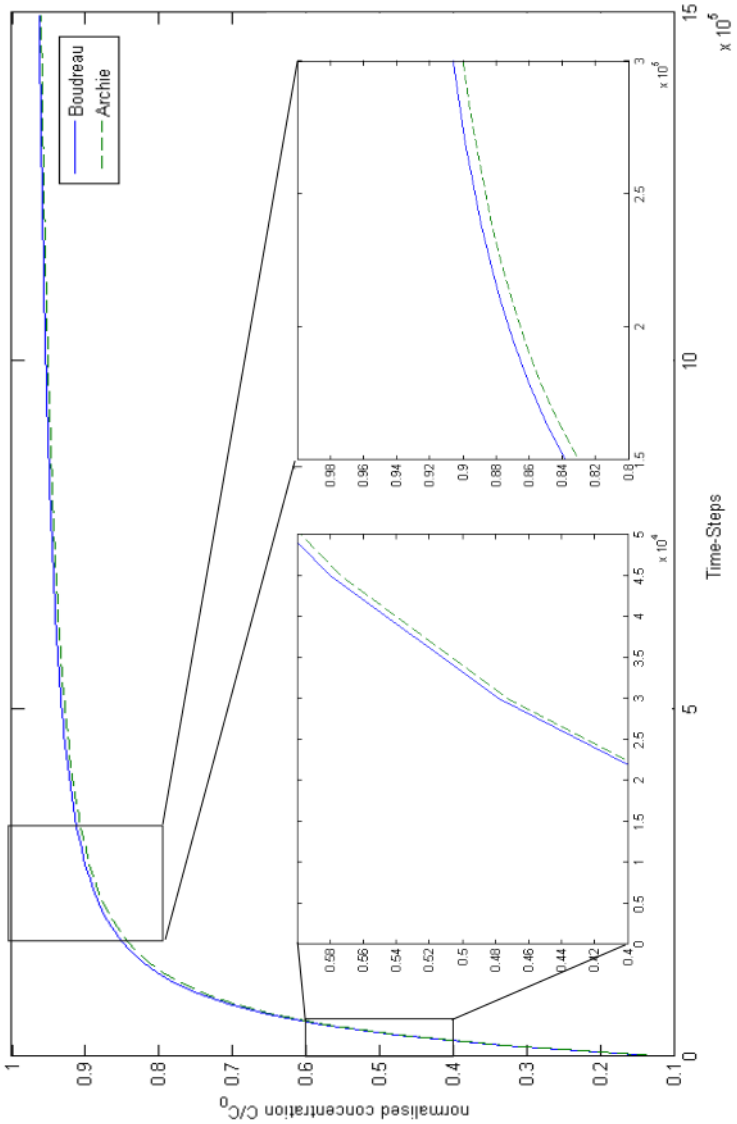

Fig. 2 Influence of the tortuosity equations on the diffusion in a sediment considering an Archie (1942) and a Boudreau (1986) tortuosity equation (respectively in dot line and solid line) with a concentration profile constant with depth in both cases.

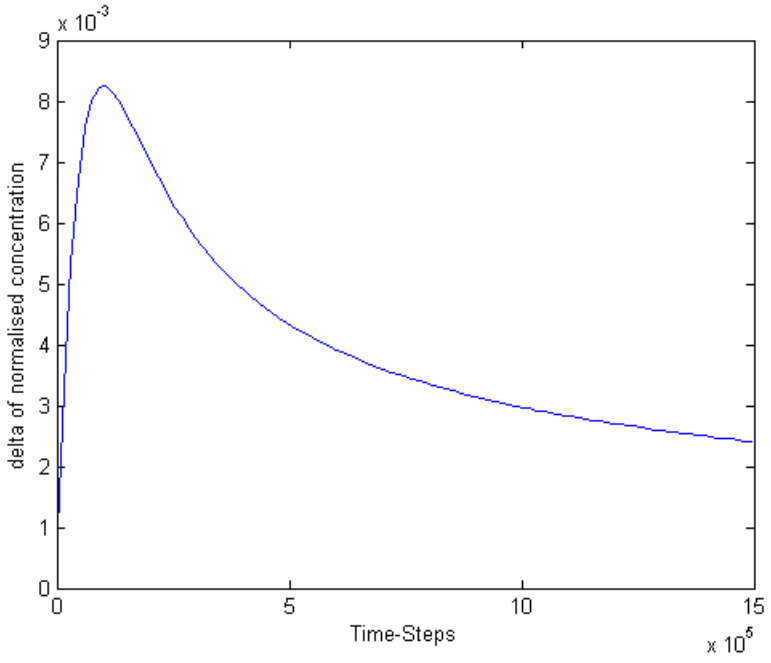

Fig. 3 Concentration delta over time between CPM_1 and CPM_2.

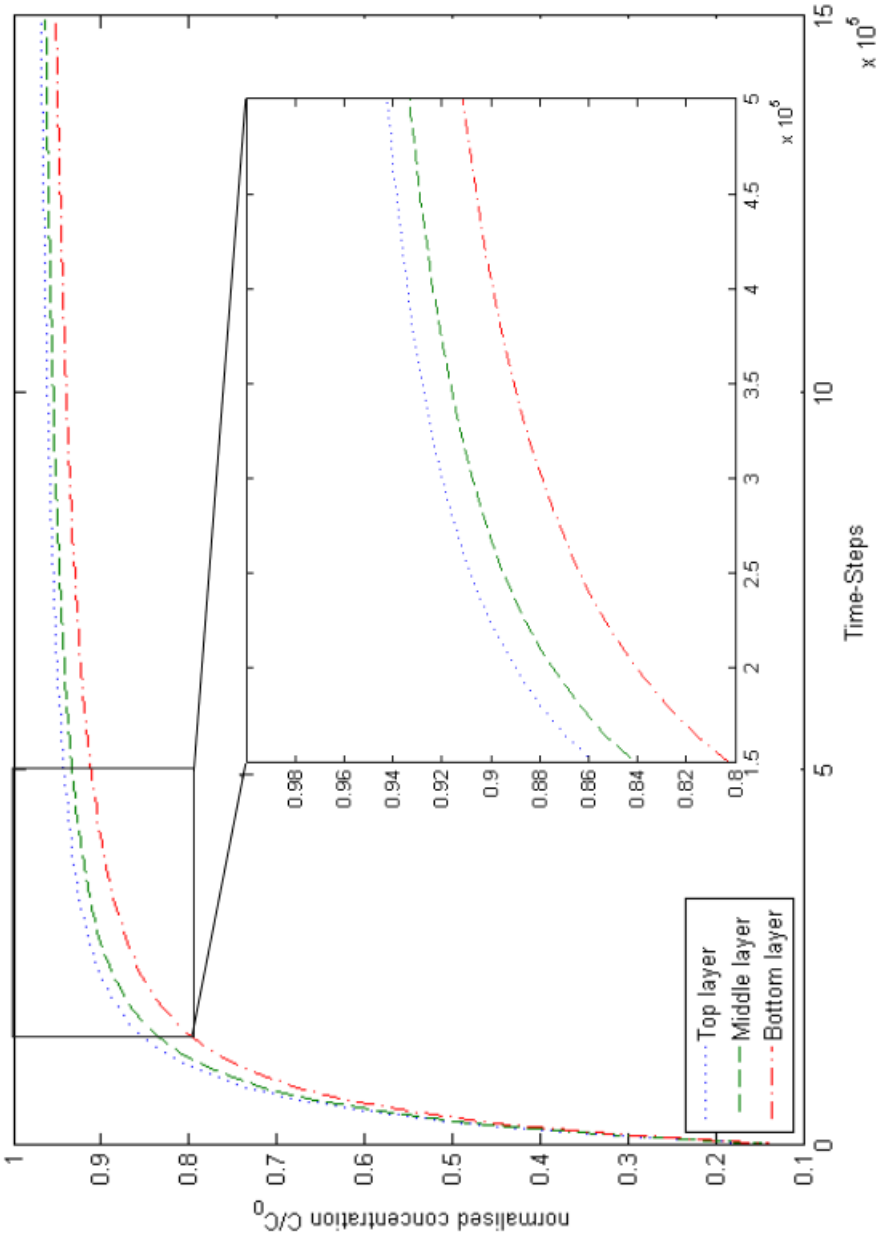

Fig. 4 Influence of the porosity on the diffusion in a sediment considering a decreasing porosity profile with depth. The diffusion for different layers is represented: a top layer (dot line), a middle layer (dash line) and a bottom layer (dot-dash line).

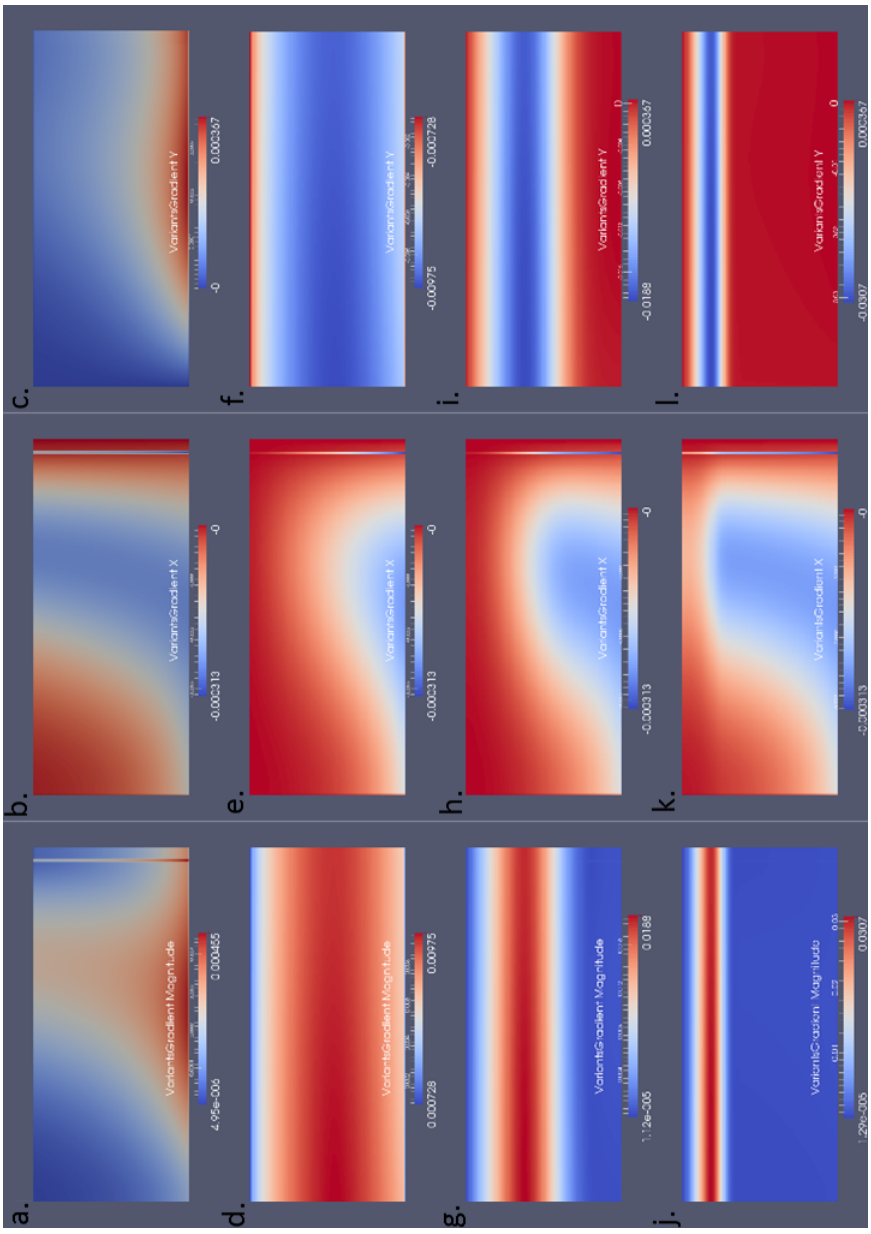

Fig. 5 Concentration gradients in the sediment represent as a vertical slice concerning VPM_1(a to c),VPM_2(d to f),VPM_3(g to i),VPM_4(j to l). For each case the gradients are representing considering the x axis (a,d,g,j), the y axis (b,e,h,k) and the magnitude (c,f,i,l) which represents the product of the gradients on both x and y.

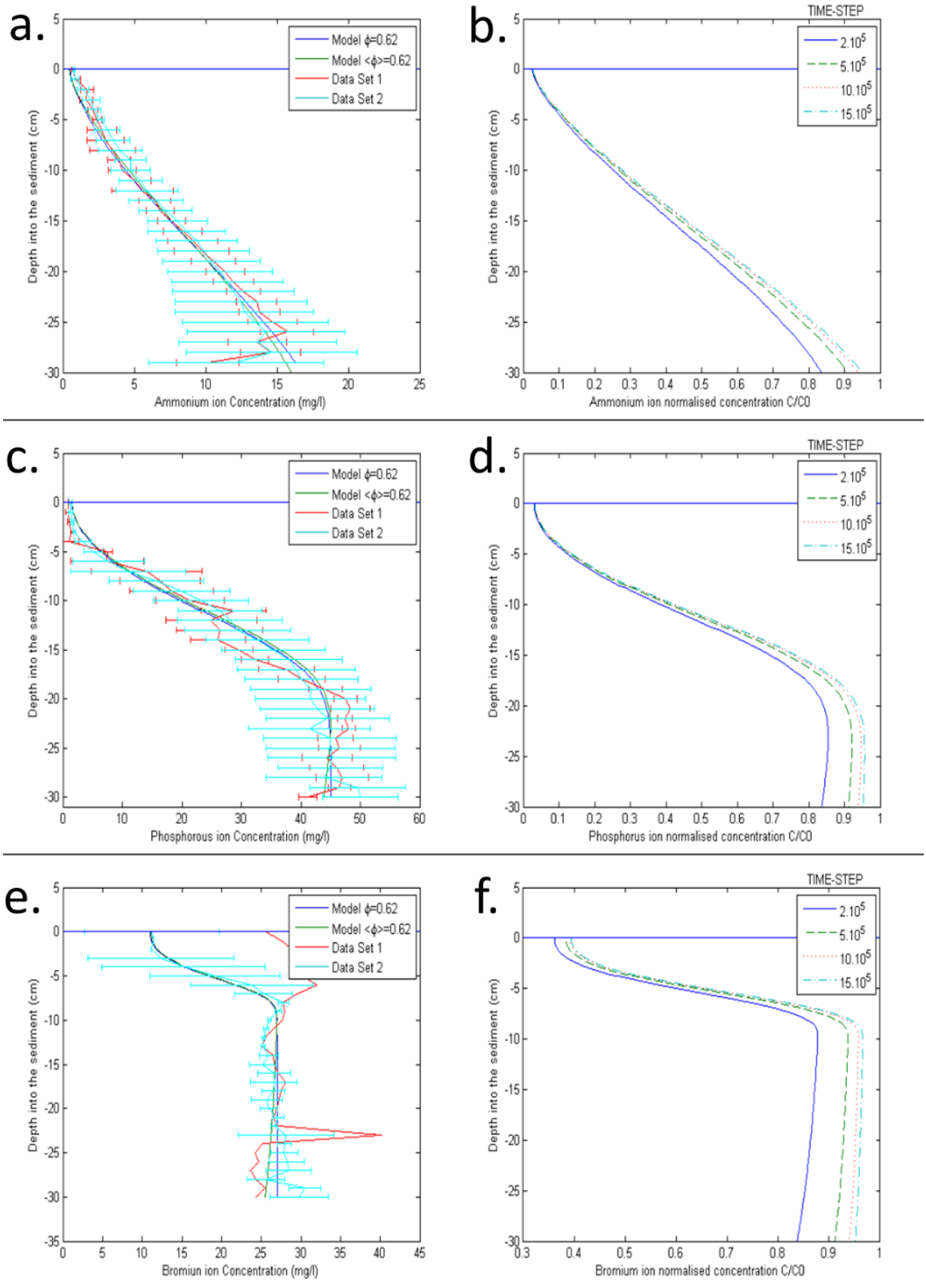

Fig. 6 Concentration profiles concerning respectively ammonium (a,b), phosphorus (c,d) and bromium (e,f). For each ion the comparison is made between Model $\phi = 0.62$ and $< \phi >= 0.62$ at full equilibration and the data obtained on the field named Data Set 1 and 2 (a,c,e). The model's simulation over 4 time-steps (b,d,f) is also represented.